11

Signaling at the Nerve-Muscle Synapse: Directly Gated Transmission

SYNAPTIC COMMUNICATION in the brain relies mainly on chemical mechanisms. Before we examine the complexities of chemical synaptic transmission in the brain, however, it will be helpful to examine the basic features of chemical synaptic transmission at the site where they were first studied and remain best understood—the nerve-muscle synapse, the junction between a motor neuron and a skeletal muscle fiber.

The nerve-muscle synapse is an ideal site for studying chemical signaling because it is relatively simple and also very accessible to experimentation. The muscle cell is large enough to accommodate the two or more microelectrodes needed to make electrical measurements. Also, the postsynaptic muscle cell is normally innervated by just one presynaptic axon, in contrast to the convergent connections on central nerve cells. Most importantly, chemical signaling at the nerve-muscle synapse involves a relatively simple mechanism. Release of neurotransmitter from the presynaptic nerve directly opens a single type of ion channel in the post-synaptic membrane.

The Neuromuscular Junction Is a Well-Studied Example of Directly Gated Synaptic Transmission

The axon of the motor neuron innervates the muscle at a specialized region of the muscle membrane called the *end-plate* (see Figure 11-1). At the region where the motor axon approaches the muscle fiber, the axon loses its myelin sheath and splits into several fine branches. The ends of the fine branches form multiple expansions or varicosities, called *synaptic boutons*, from which the motor neuron releases its transmitter (Figure 11–1). Each bouton is positioned over a *junctional fold*, a deep depression in the surface of the postsynaptic muscle fiber that contains the transmitter receptors (Figure 11–2). The transmitter released by the axon terminal is acetylcholine (ACh), and the receptor on the muscle mem-

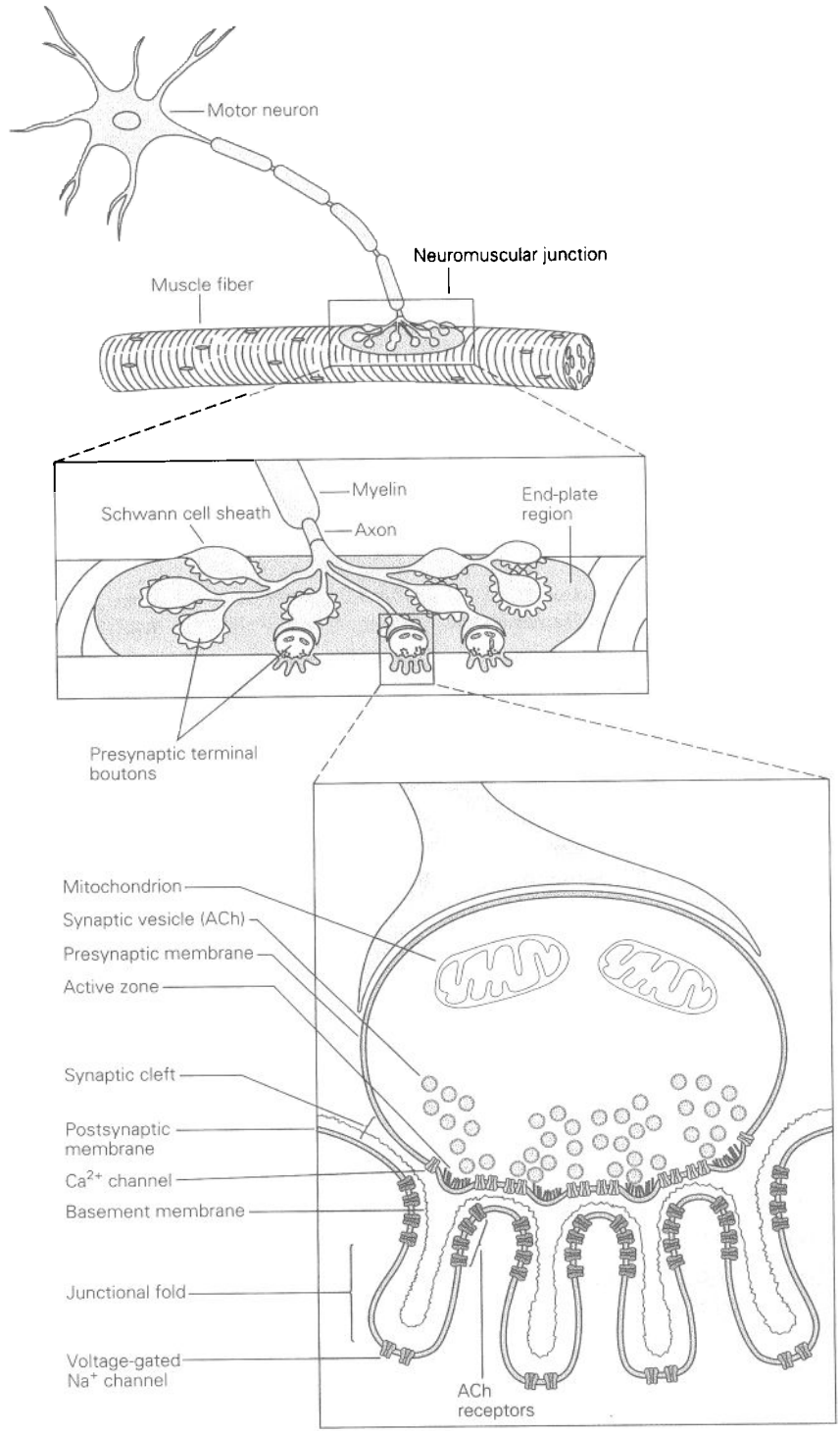

Figure 11-1 The neuromuscular junction is readily visible with the light microscope. At the muscle the motor axon ramifies into several fine branches approximately 2 μm thick. Each branch forms multiple swellings called presynaptic boutons, which are covered by a thin layer of Schwann cells. The boutons lie over a specialized region of the muscle fiber membrane, the *end-plate,* and are separated from the muscle membrane by a 100 nm *synaptic cleft.* Each presynaptic bouton contains mitochondria and synaptic vesicles clustered around *active zones,* where the acetylcholine (ACh) transmitter is released. Immediately under each bouton in the end-plate are several *junctional folds,* which contain a high density of ACh receptors at their crests. The muscle fiber is covered by a layer of connective tissue, the *basement membrane* (or basal lamina), consisting of collagen and glycoproteins. Both the presynaptic terminal and the muscle fiber secrete proteins into the basement membrane, including the enzyme acetylcholinesterase, which inactivates the ACh released from the presynaptic terminal by breaking it down into acetate and choline. The basement membrane also organizes the synapse by aligning the presynaptic boutons with the postsynaptic junctional folds. (Adapted in part from McMahan and Kuffler 1971.)

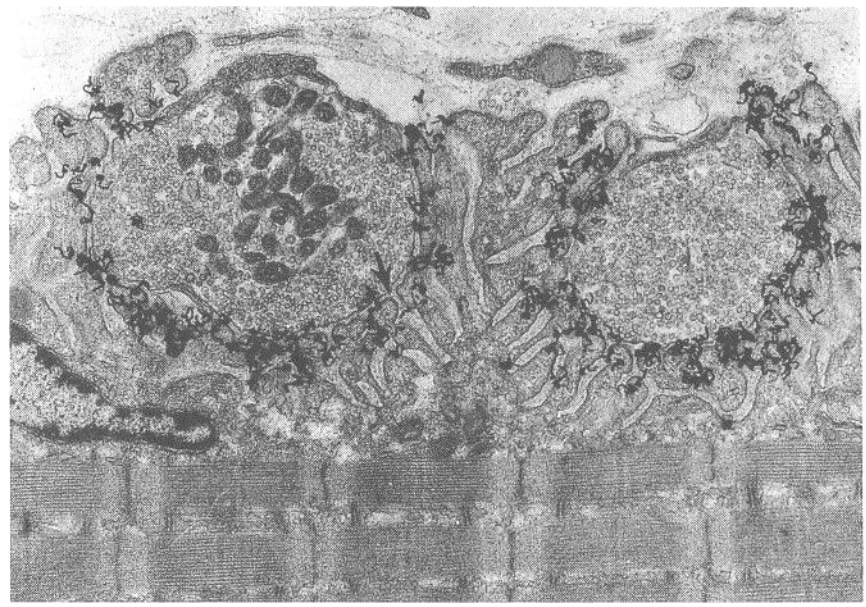

Figure 11-2 Electron microscope autoradiograph of the vertebrate neuromuscular junction, showing localization of ACh receptors (black developed grains) at the top one-third of the postsynaptic junctional folds. This receptor-rich region is characterized by an increased density of the postjunctional membrane (**arrow**). The membrane was incubated with radiolabeled α-bungarotoxin, which binds to the ACh receptor. Radioactive decay results in the emittance of a radioactive particle, causing silver grains to become fixed (**dark grains**). Magnification × 18,000.

brane is the nicotinic type of ACh receptor (Figure 11–3).[1]

The presynaptic and postsynaptic membranes are separated by a synaptic cleft around 100 nm wide. Within the cleft is a basement membrane composed of collagen and other extracellular matrix proteins. The enzyme acetylcholinesterase, which rapidly hydrolyzes ACh, is anchored to the collagen fibrils of the basement membranes. In the muscle cell, in the region below the crest of the junctional fold and extending into the fold, the membrane is rich in voltage-gated Na^+ channels.

Each presynaptic bouton contains all the machinery required to release neurotransmitter. This includes the *synaptic vesicles*, which contain the transmitter ACh, and the *active zone*, a part of the membrane specialized for vesicular release of transmitter (see Figure 11-1). Every active zone in the presynaptic membrane is positioned opposite a junctional fold in the postsynaptic cell. At the crest of each fold the receptors for ACh are clustered in a lattice, with a density of about 10,000 receptors per square micrometer (Figures 11-2 and 11-3). In addition, each active zone contains voltage-gated Ca^{2+} channels that permit Ca^{2+} to enter the terminal with each action potential (see Figure 11-1). This influx of Ca^{2+} triggers fusion of the synaptic vesicles in the active zones with the plasma membrane, and fusion leads to release of the vesicle's content into the synaptic cleft.

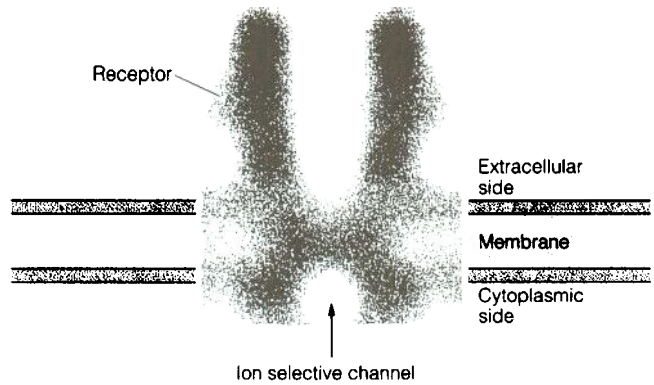

Figure 11-3 Reconstructed electron microscope image of the ACh receptor-channel complex in the fish *Torpedo californica*. The image was obtained by computer processing of negatively stained images of ACh receptors. The resolution is 1.7 nm, fine enough to see overall structures but too coarse to resolve individual atoms. The overall diameter of the receptor and its channel is about 8.5 nm. The pore is wide at the external and internal surfaces of the membrane but narrows considerably within the lipid bilayer. The channel extends some distance into the extracellular space. (Adapted from Toyoshima and Unwin 1988.)

[1] There are two basic types of receptors for ACh: nicotinic and muscarinic. The nicotinic receptor is an ionotropic receptor while the muscarinic receptor is a metabotropic receptor (see Chapter 10). The two receptors can be distinguished further because certain drugs that simulate the actions of ACh—that is, nicotine and muscarine—bind exclusively to one or the other type of ACh receptor. We shall learn about muscarinic ACh receptors in Chapter 13.

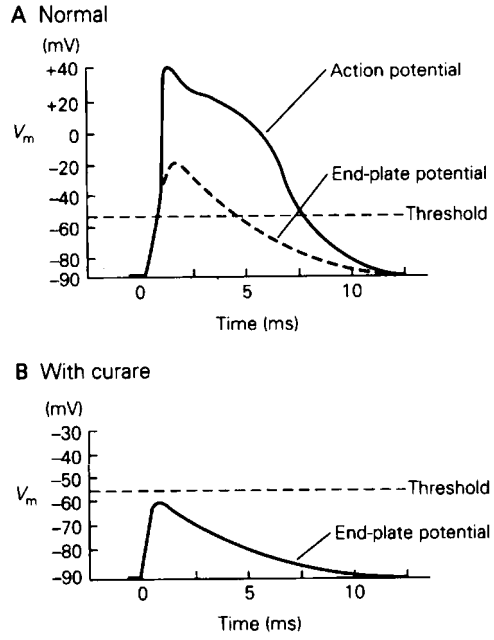

Figure 11-4 The end-plate potential can be isolated pharmacologically for study.

A. Under normal circumstances stimulation of the motor axon produces an action potential in a skeletal muscle cell. The **dashed line** shows the inferred time course of the end-plate potential that triggers the action potential.

B. The end-plate potential can be isolated in the presence of curare, which blocks the binding of ACh to its receptor and so prevents the end-plate potential from reaching the threshold for an action potential (**dashed line**). In this way the currents and channels that contribute to the end-plate potential, which are different from those producing an action potential, can be studied. The values for the resting potential (−90 mV), end-plate potential, and action potential shown in these intracellular recordings are typical of a vertebrate skeletal muscle.

The Motor Neuron Excites the Muscle by Opening Ion Channels at the End-Plate

Upon release of ACh from the motor nerve terminal, the membrane at the end-plate depolarizes rapidly. The excitatory postsynaptic potential in the muscle cell is called the *end-plate potential*. The amplitude of the end-plate potential is very large; stimulation of a single motor cell produces a synaptic potential of about 70 mV. This change in potential usually is large enough to rapidly activate the voltage-gated Na^+ channels in the junctional folds. This converts the end-plate potential into an action potential, which propagates along the muscle fiber. (In contrast, in the central nervous system most presynaptic neurons produce postsynaptic potentials less than 1 mV in amplitude, so that input from many presynaptic neurons is needed to generate an action potential there.)

The Synaptic Potential at the End-Plate Is Produced by Ionic Current Flowing Through Acetylcholine-Gated Channels

The end-plate potential was first studied in detail in the 1950s by Paul Fatt and Bernard Katz using intracellular voltage recordings. Fatt and Katz were able to isolate the end-plate potential using the drug curare[2] to reduce the amplitude of the end-plate potential below the threshold for the action potential (Figure 11-4). They found that the synaptic potential in muscle cells was largest at the end-plate, decreasing progressively with distance from the end-plate region (Figure 11-5). They concluded that the synaptic potential is generated by an inward ionic current confined to the end-plate region, which then spreads passively away from the end-plate. (Remember, an inward current corresponds to an influx of positive charge, which will depolarize the inside of the membrane.) Current flow is confined to the end-plate because the ACh-activated ion channels are localized there, opposite the presynaptic terminal from which transmitter is released.

The synaptic potential at the end-plate rises rapidly but decays more slowly. The rapid rise is due to the sudden release of ACh into the synaptic cleft by an action potential in the presynaptic nerve terminal. Once released, ACh diffuses rapidly to the receptors at the end-plate. Not all the ACh reaches postsynaptic receptors, however, because it is quickly removed from the synaptic cleft by two processes: hydrolysis and diffusion out of the synaptic cleft.

The current that generates the end-plate potential was first studied in voltage-clamp experiments (see Box 9-1). These studies revealed that the end-plate current rises and decays more rapidly than the resultant end-plate potential (Figure 11-6). The time course of the end-plate current is directly determined by the rapid opening and closing of the ACh-gated ion channels. Because it takes time for an ionic current to charge or discharge the muscle membrane capacitance, and thus alter the membrane voltage, the end-plate potential lags behind the synaptic current (see Figure 8-3 and the Postscript at the end of this chapter).

[2] Curare is a mixture of plant toxins used by South American Indians, who apply it to arrowheads to paralyze their quarry. Tubocurarine, the purified active agent, blocks neuromuscular transmission by binding to the nicotinic ACh receptor, preventing its activation by ACh.

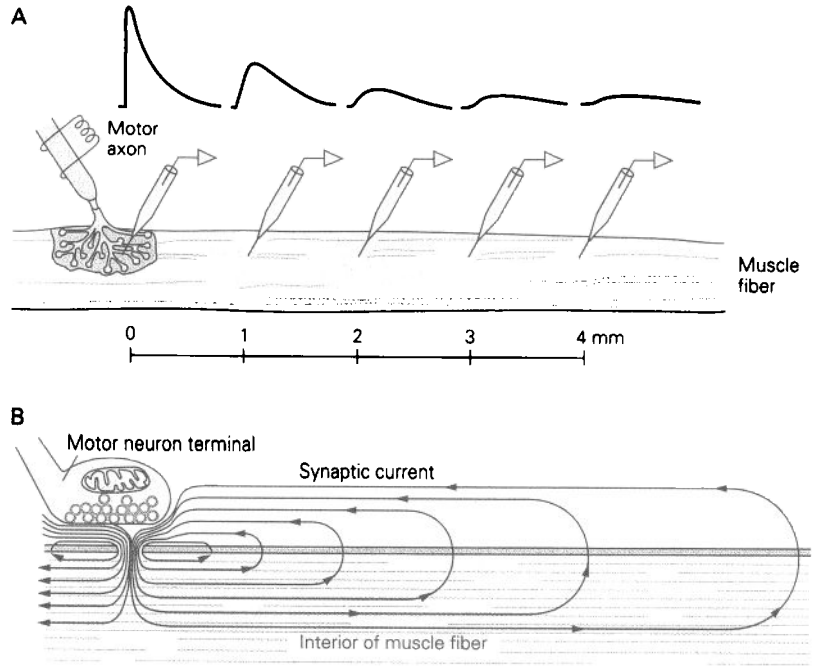

Figure 11-5 The synaptic potential in muscle is largest at the end-plate region and passively propagates away from it. (Adapted from Miles 1969.)

A. The amplitude of the synaptic potential decays and the time course of the potential slows with distance from the site of initiation in the end-plate.

B. The decay results from leakiness of the muscle fiber membrane. Since current flow must complete a circuit, the inward synaptic current at the end-plate gives rise to a return flow of outward current through resting channels and across the membrane (the capacitor). It is this return flow of outward current that produces the depolarization. Since current leaks out all along the membrane, the current flow decreases with distance from the end-plate. Thus, unlike the regenerative action potential, the local depolarization produced by the synaptic potential of the membrane decreases with distance.

The Ion Channel at the End-Plate Is Permeable to Both Sodium and Potassium

Why does the opening of the ACh-gated ion channels lead to an inward current flow that produces the depolarizing end-plate potential? And which ions move through the ACh-gated ion channels to produce this inward current? One important clue to the identity of the ion (or ions) responsible for the synaptic current can be obtained from experiments that measure the value of the chemical driving force propelling ions through the channel. Remember, from Chapter 7, the current flow through a membrane conductance is given by the product of the membrane conductance and the electrochemical driving force on the ions conducted through the channels. The end-plate current that underlies the excitatory postsynaptic potential (EPSP) is defined as

$$I_{EPSP} = g_{EPSP} \times (V_m - E_{EPSP}), \qquad \textbf{(11-1)}$$

where I_{EPSP} is the end-plate current, g_{EPSP} is the conductance of the ACh-gated channels, V_m is the membrane potential, and E_{EPSP} is the chemical driving force, or battery, that results from the concentration gradients of the ions conducted through the ACh-gated channels. The fact that current flowing through the end-plate is inward at the normal resting potential of a muscle cell (−90 mV) indicates that there is an inward (negative) electrochemical driving force on the ions that carry current through the ACh-gated channels at this potential. Thus, E_{EPSP} must be positive to −90 mV.

From Equation 11-1 we see that the value of E_{EPSP} can be determined by altering the membrane potential in a voltage-clamp experiment and determining its effect on the synaptic current. Depolarizing the membrane reduces the net inward electrochemical driving force, causing a decrease in the magnitude of the inward end-plate current. If the membrane potential is set equal to the value of the battery representing the chemical driving force (E_{EPSP}), no net synaptic current will flow through the end-plate because the electrical driving force (due to V_m) will exactly balance the chemical driving force (due to E_{EPSP}). The potential at which the net ionic current is zero is the *reversal potential* for current flow through the synaptic channels. By determining the reversal potential we can experimentally measure the value of E_{EPSP}, the chemical force driving ions through the ACh-gated channels at the end-plate. If the membrane potential is made more positive than E_{EPSP}, there will be a net outward driving force. In this case stimulation of the motor nerve leads to an outward ionic current, by opening the ACh-gated channels, and this outward ionic current hyperpolarizes the membrane.

If an influx of Na^+ were solely responsible for the end-plate potential, the reversal potential for the excitatory postsynaptic potential would be the same as the equilibrium potential for Na^+, or +55 mV. Thus, if the membrane potential is experimentally altered from −100 to +55 mV, the end-plate current should diminish progressively because the electrochemical driving force

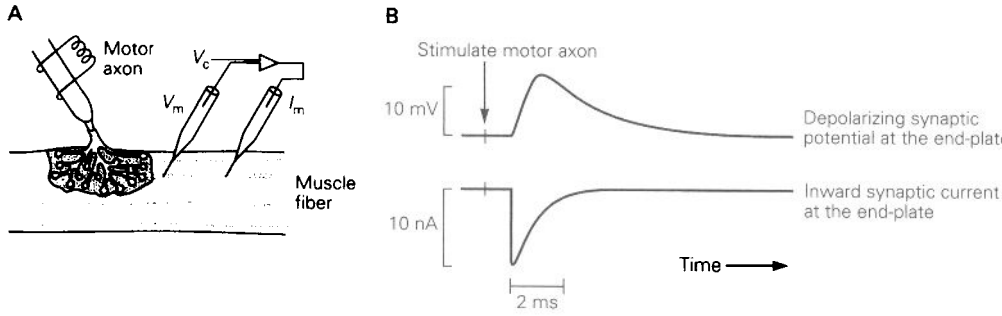

Figure 11-6 The end-plate current rises and decays more rapidly than the end-plate potential.

A. The membrane at the end-plate is voltage-clamped by inserting two microelectrodes into the muscle at the end-plate. One electrode measures membrane voltage (V_m) and the second passes current (I_m). Both electrodes are connected to a feedback amplifier, which ensures that the proper amount of current (I_m) is delivered so that V_m will be clamped at the command potential V_c. The synaptic current evoked by stimulating the motor nerve can then be measured at a constant membrane potential, for example −90 mV (see Box 9-1).

B. The end-plate potential, measured when the voltage clamp is not active, changes relatively slowly, following in time the inward synaptic current measured under voltage-clamp conditions. This is because synaptic current must first alter the charge on the membrane capacitance of the muscle before the muscle membrane is depolarized (see Chapter 8 and Postscript in this chapter).

on Na^+ ($V_m - E_{Na}$) is reduced. At +55 mV the inward current flow should be abolished, and at potentials more positive than +55 mV the end-plate current should reverse in direction and flow outward.

Instead experiments at the end-plate showed that as the membrane potential is reduced, the inward current rapidly becomes smaller and is abolished at 0 mV! At values more positive than 0 mV the end-plate current reverses direction and begins to flow outward (Figure 11-7). This particular value of membrane potential is not equal to the equilibrium potential for Na^+, or for that matter any of the major cations or anions. In fact, this potential is produced not by a single ion species but by a combination of ions. The synaptic channels at the end-plate are almost equally permeable to both major cations, Na^+ and K^+. Thus, during the end-plate potential Na^+ flows into the cell and K^+ flows out. The reversal potential is at 0 mV because this is a weighted average of the equilibrium potentials for Na^+ and K^+ (Box 11-1). At the reversal potential the influx of Na^+ is balanced by an equal efflux of K^+.

Why are the ACh-gated channels at the end-plate not selective for a single ion species like the voltage-gated channels selective for either Na^+ or K^+? The pore diameter of the ACh-gated channel is thought to be substantially larger than that of the voltage-gated channels. Electrophysiological measurements suggest that the pore may be up to 0.8 nm in diameter in mammals. This estimate is based on the size of the largest organic cation that can permeate the channel. For example, the permeant cation tetramethylammonium (TMA) is around 0.6 nm in diameter. In contrast, the voltage-gated Na^+ channel is only permeant to organic cations that are smaller than 0.5 × 0.3 nm in cross section, and voltage-gated K^+ channels will only conduct ions less than 0.3 nm in diameter. The relatively large diameter of the ACh pore is thought to provide a water-filled environment that allows cations to diffuse through the channel, much as they would in free solution. This explains why the pore does not discriminate between Na^+ and K^+. It also explains why even divalent cations, such as Ca^{2+}, can permeate the channel. Anions are excluded, however, by the presence of fixed negative charges in the channel, as described later in this chapter.

The Current Flow Through Single Ion Channels Can Be Measured by the Patch Clamp

The current for an end-plate potential flows through several hundred thousand channels. Recordings of the current flow through single ACh-gated ion channels, using the patch clamp technique (see Box 6-1), have provided us with insight into the molecular events underlying the end-plate potential. Before the introduction of the patch clamp physiologists held two opposing views as to what the time course of the single-channel current should look like. Some thought that the single-channel currents were a microscopic version of the end-plate current recorded with the voltage clamp, having a rapid

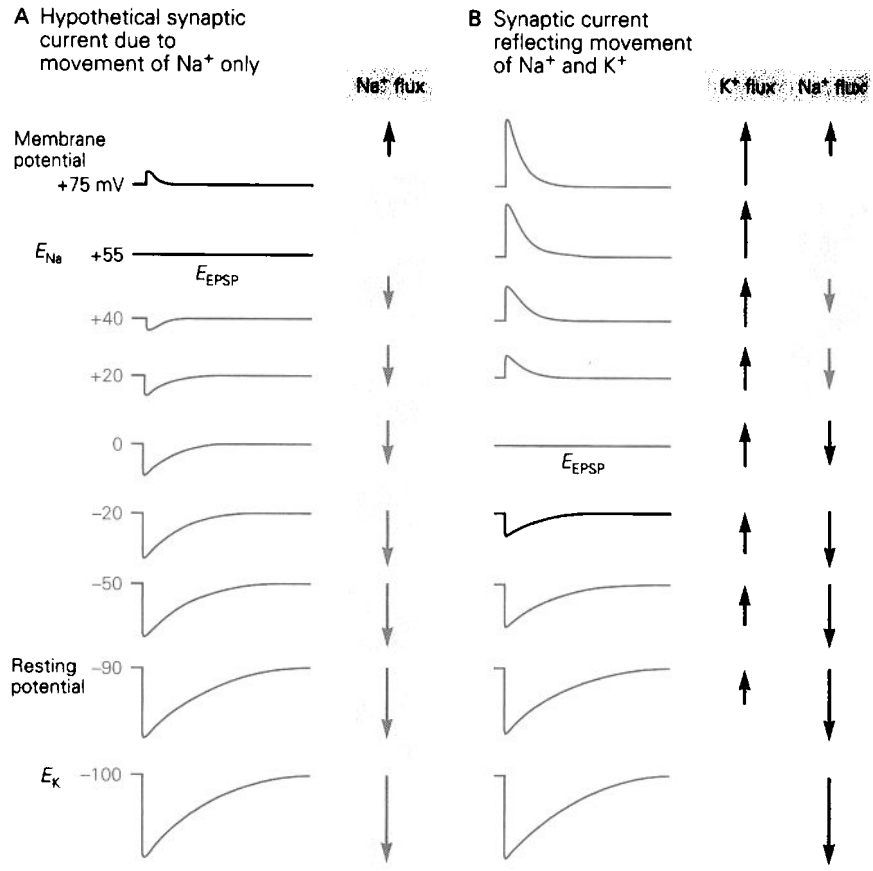

Figure 11-7 The end-plate potential is produced by the simultaneous flow of Na^+ and K^+ through the same ACh-gated channels.

A. The ionic currents responsible for the end-plate potential can be determined by measuring the reversal potential of the end-plate current. The voltage of the muscle membrane is clamped at different potentials, and the synaptic current is measured when the nerve is stimulated. If Na^+ flux alone were responsible for the end-plate current, the reversal potential would occur at +55 mV, the equilibrium potential for Na^+ (E_{Na}). The arrow next to each current record reflects the magnitude of the net Na^+ flux at that membrane potential.

B. The end-plate current actually reverses at 0 mV because the ion channel is permeable to both Na^+ and K^+, which are able to move into and out of the cell simultaneously (see Box 11-1). The net current is the sum of the Na^+ and K^+ fluxes through the end-plate channels. At the reversal potential (E_{EPSP}) the inward Na^+ flux is balanced by an outward K^+ flux so that no net current flows.

rising phase and a more slowly decaying falling phase. Others thought that the channels opened in an all-or-none manner, producing step-like currents similar to that seen with gramicidin (see Chapter 6).

Individual Acetylcholine-Gated Channels Conduct a Unitary Current

The first successful recordings of single ACh-gated channels from skeletal muscle cells, by Erwin Neher and Bert Sakmann in 1976, showed that the channels open and close in a step-like manner, generating very small rectangular steps of ionic current (Figure 11-8). At a constant membrane potential a channel generates a similar-size current pulse each time it opens. At a resting potential of −90 mV the current steps are around −2.7 pA in amplitude. Although this is a very small current, it corresponds to a flow through an open channel of around 17 million ions per second!

The unitary current steps change in size with membrane potential. This is because the single-channel current depends on the electrochemical driving force ($V_m - E_{EPSP}$). Recall that Ohm's law applied to synaptic current is

$$I_{EPSP} = g_{EPSP} \times (V_m - E_{EPSP}).$$

For single ion channels the equivalent expression is

$$i_{EPSP} = \gamma_{EPSP} \times (V_m - E_{EPSP}),$$

where i_{EPSP} is the amplitude of current flow through one channel and γ_{EPSP} is the conductance of a single channel. The relationship between i_{EPSP} and membrane voltage is linear, indicating that the single-channel conductance is constant and does not depend on membrane voltage; that is, the channel behaves as a simple resistor. From the slope of this relation the channel is found to have a conductance of 30 pS. The reversal potential of 0 mV, obtained from the intercept of the voltage axis, is identical to that for the end-plate current (Figure 11-9).

Although the amplitude of the current flowing through a single ACh channel is constant from opening

Box 11-1 Reversal Potential of the End-Plate Potential

The reversal potential of a membrane current carried by more than one ion species, such as the end-plate current through the ACh-gated channel, is determined by two factors: (1) the relative conductance for the permeant ions (g_{Na} and g_K in the case of the end-plate current) and (2) the equilibrium potentials of the ions (E_{Na} and E_K).

At the reversal potential for the ACh-gated current, inward current carried by Na^+ is balanced by outward current carried by K^+:

$$I_{Na} + I_K = 0. \quad \textbf{(11-2)}$$

The individual Na^+ and K^+ currents can be obtained from

$$I_{Na} = g_{Na} \times (V_m - E_{Na}) \quad \textbf{(11-3a)}$$

and

$$I_K = g_K \times (V_m - E_K). \quad \textbf{(11-3b)}$$

Remember that these currents do not result from Na^+ and K^+ flowing through separate channels (as occurs during the action potential) but represent Na^+ and K^+ movement through the same ACh-gated channel. Since at the reversal potential $V_m = E_{EPSP}$, we can substitute Equations 11-3a and 11-3b for I_{Na} and I_K in Equation 11-2:

$$g_{Na} \times (E_{EPSP} - E_{Na}) + g_K \times (E_{EPSP} - E_K) = 0. \quad \textbf{(11-4)}$$

Solving this equation for E_{EPSP} yields

$$E_{EPSP} = \frac{(g_{Na} \times E_{Na}) + (g_K \times E_K)}{g_{Na} + g_K}. \quad \textbf{(11-5)}$$

If we divide the top and bottom of the right side of this equation by g_K, we obtain

$$E_{EPSP} = \frac{E_{Na}(g_{Na}/g_K) + E_K}{(g_{Na}/g_K) + 1}. \quad \textbf{(11-6)}$$

Thus, if $g_{Na} = g_K$, then $E_{EPSP} = (E_{Na} + E_K)/2$.

These equations can also be used to solve for the ratio g_{Na}/g_K if one knows E_{EPSP}, E_K, and E_{Na}. Thus, rearranging Equation 11-4 yields

$$\frac{g_{Na}}{g_K} = \frac{E_{EPSP} - E_K}{E_{Na} - E_{EPSP}}. \quad \textbf{(11-7)}$$

At the neuromuscular junction $E_{EPSP} = 0$ mV, $E_K = -100$ mV, and $E_{Na} = +55$ mV. Thus, from Equation 4, g_{Na}/g_K has a value of approximately 1.8, indicating that the conductance of the ACh-gated channel for Na^+ is slightly higher than for K^+. A comparable approach can be used to analyze the reversal potential and the movement of ions during excitatory and inhibitory synaptic potentials in central neurons (Chapter 12).

to opening, the duration of openings and the time between openings of an individual channel vary considerably. These variations occur because channel openings and closings are stochastic. They obey the same statistical law that describes radioactive decay. Because of the random thermal motions and fluctuations that a channel experiences, it is impossible to predict exactly how long it will take any one channel to encounter ACh or how long that channel will stay open before the ACh dissociates and the channel closes. However, the average length of time a particular type of channel stays open is a well-defined property of that channel, just as the half-life of radioactive decay is an invariant property of a particular isotope. The mean open time for ACh-gated channels is around 1 ms. Thus each channel opening is associated with the movement of about 17,000 ions.

Unlike the voltage-gated channels, the ACh-gated channels are not opened by membrane depolarization. Instead a ligand (ACh) causes the channels to open. Each channel is thought to have two binding sites for ACh; to open, a channel must bind two molecules of ACh. Once a channel closes, the ACh molecules dissociate and the channel remains closed until it binds ACh again.

Four Factors Determine the End-Plate Current

Stimulation of a motor nerve releases a large quantity of ACh into the synaptic cleft. The ACh rapidly diffuses across the cleft and binds to the ACh receptors, causing more than 200,000 ACh receptor-channels to open almost simultaneously. (This number is obtained by comparing the total end-plate current, around −500 nA, with the current through a single ACh-gated channel, around −2.7 pA). How do small step-like changes in current flowing through 200,000 individual ACh-gated channels produce the smooth waveform of the end-plate current?

The rapid and large rise in ACh concentration upon stimulation of the motor nerve causes a large increase in the total conductance of the end-plate membrane, g_{EPSP}, and produces the rapid rise in end-plate current (Figure 11-10). The ACh in the cleft falls to zero rapidly (in less than 1 ms) because of enzymatic hydrolysis and diffusion. After the fall in ACh concentration, the channels begin to close in the random manner described above. Each closure produces a small step-like decrease in end-plate current because of the all-or-none nature of single-channel currents. However, since each unitary current step is

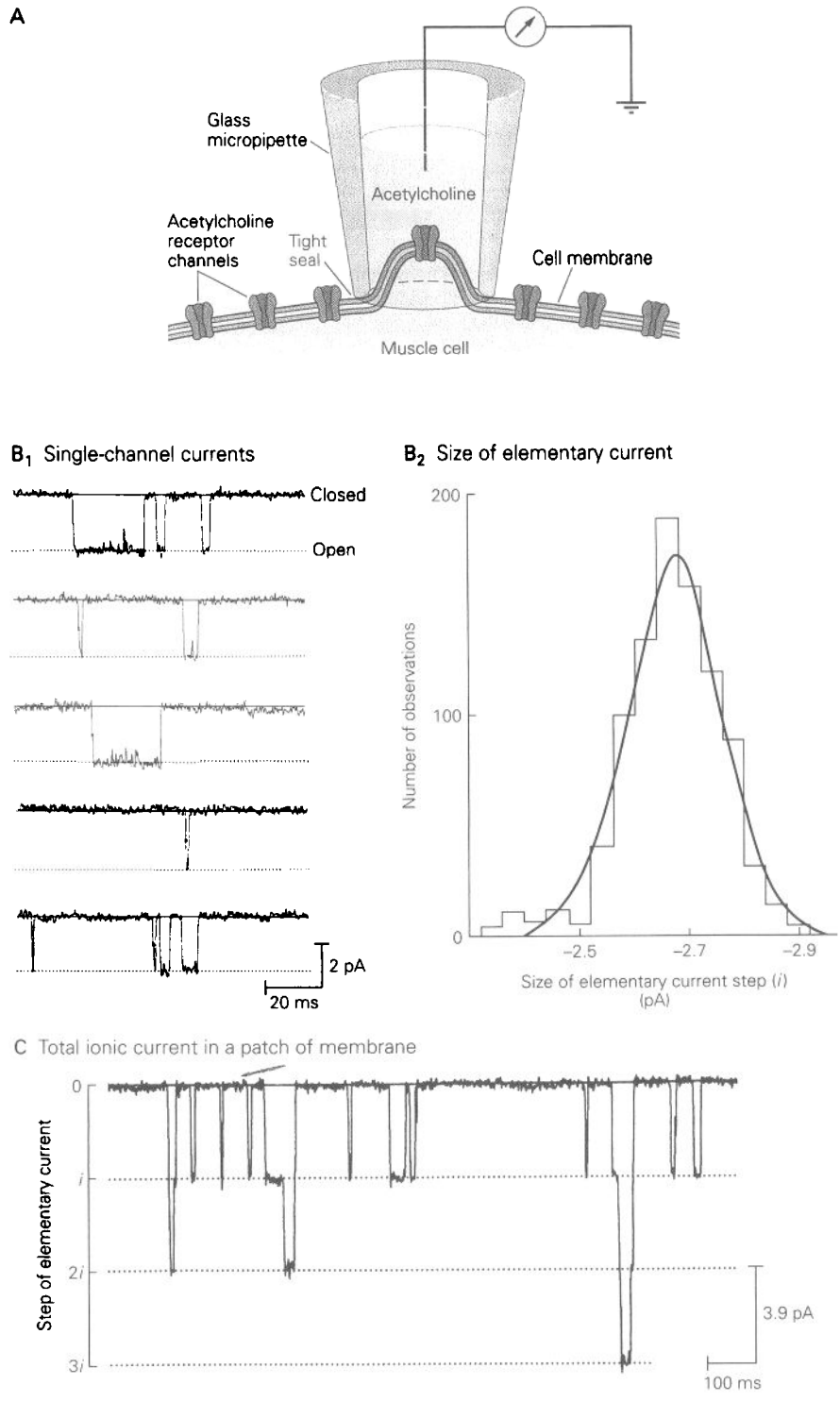

Figure 11-8 Individual ACh-gated channels open in an all-or-none fashion.

A. The patch-clamp technique is used to record currents from single ACh-gated channels. The patch electrode is filled with salt solution that contains a low concentration of ACh and is then brought into close contact with the surface of the muscle membrane (see Box 6-1).

B. Single-channel currents from a patch of membrane on a frog muscle fiber were recorded in the presence of 100 nM ACh at a resting membrane potential of −90 mV. **1.** The opening of a channel results in the flow of inward current (recorded as a downward step). The patch contained a large number of ACh-gated channels so that successive openings in the record probably arise from distinct channels. **2.** A histogram of the amplitudes of these rectangular pulses has a single peak. This distribution indicates that the patch of membrane contains only a single type of active channel and that the size of the elementary current through this channel varies randomly around a mean of −2.7 pA (1 pA = 10^{-12} A). This mean, the *elementary current,* is equivalent to an elementary conductance of about 30 pS. (Courtesy of B. Sakmann.)

C. When the membrane potential is increased to −130 mV, the individual channel currents give rise to all-or-none increments of −3.9 pA, equivalent to 30 pS. Sometimes more than one channel opens simultaneously. In this case, the individual current pulses add linearly. The record shows one, two, or three channels open at different times in response to transmitter. (Courtesy of B. Sakmann.)

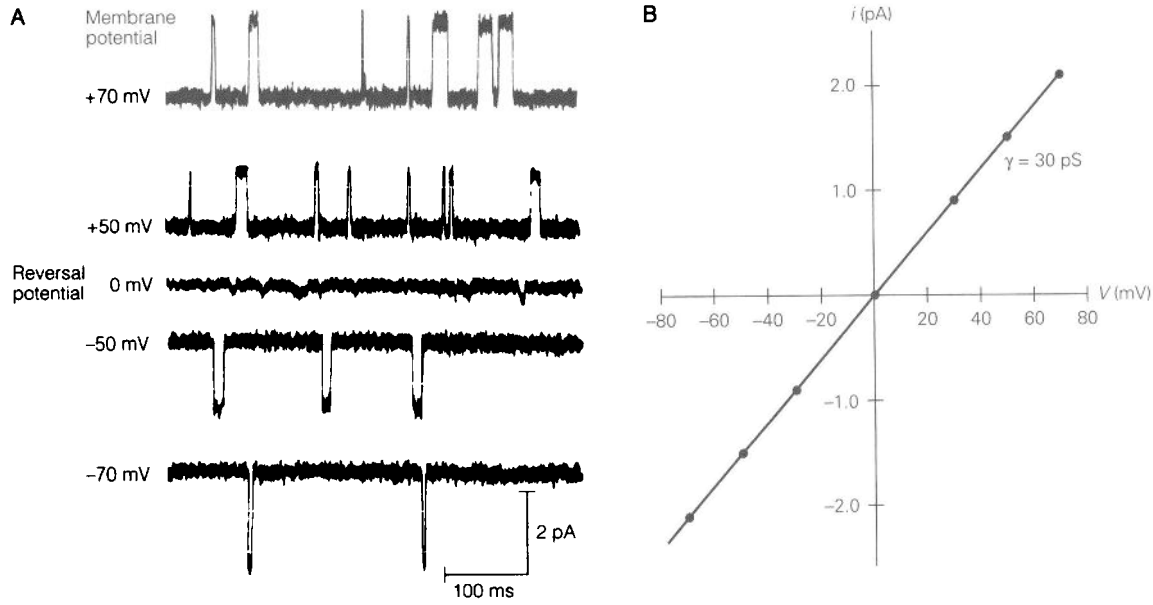

Figure 11-9 Single open ACh-gated channels behave as simple resistors.

A. The voltage across a patch of membrane was systematically varied during exposure to 2 μM ACh. The current recorded at the patch is inward at voltages negative to 0 mV and outward at voltages positive to 0 mV, defining the reversal potential for the channels.

B. The current flow through a single ACh-activated channel depends on membrane voltage. The linear relation shows that the channel behaves as a simple resistor with a conductance of about 30 pS.

tiny relative to the large current carried by many thousands of channels, the random closing of a large number of small unitary currents causes the total end-plate current to appear to decay smoothly (Figure 11-10).

The summed conductance of all open channels in a large population of ACh channels is the total synaptic conductance, $g_{EPSP} = n \times \gamma$, where n is the average number of channels opened by the ACh transmitter and γ is the conductance of a single channel. For a large number of ACh channels, $n = N \times p_o$, where N is the total number of ACh channels in the end-plate membrane and p_o is the probability that any given ACh channel is open. The probability that a channel is open depends largely on the concentration of the transmitter at the receptor, not on the value of the membrane potential, because the channels are opened by the binding of ACh, not by voltage. The total end-plate current is therefore given by

$$I_{EPSP} = N \times p_o \times \gamma \times (V_m - E_{EPSP})$$

or

$$I_{EPSP} = n \times \gamma \times (V_m - E_{EPSP}).$$

This equation shows that the current for the end-plate potential depends on four factors: (1) the total number of end-plate channels (N); (2) the probability that a channel is open (p_o); (3) the conductance of each open channel (γ); and (4) the driving force that acts on the ions ($V_m - E_{EPSP}$).

The relationships between single-channel current, total end-plate current, and end-plate potential are shown in Figure 11-11 for a wide range of membrane potentials.

The Molecular Properties of the Acetylcholine-Gated Channel at the Nerve-Muscle Synapse Are Known

Ligand-Gated Channels for Acetylcholine Differ From Voltage-Gated Channels

Ligand-gated channels such as the ACh-gated channels that produce the end-plate potential differ in two important ways from the voltage-gated channels that generate the action potential at the neuromuscular junction. First, two distinct classes of voltage-gated channels are activated sequentially to generate the action potential, one selective for Na^+ and the other for K^+. In contrast, the ACh-gated channel alone generates end-plate potentials, and it allows both Na^+ and K^+ to pass with nearly equal permeability.

A second difference between ACh-gated and voltage-gated channels is that Na^+ flux through voltage-gated channels is regenerative: the increased depolarization of the cell caused by the Na^+ influx opens more voltage-gated Na^+ channels. This regenerative feature is responsible for the all-or-none property of the action potential. In contrast, the number of ACh-activated channels opened during the synaptic potential varies according to the amount of ACh available. The depolarization produced by Na^+ influx through these channels does not lead to the opening of more transmitter-gated channels; it is therefore limited and by itself cannot produce an action potential. To trigger an action potential, a synaptic potential must recruit neighboring voltage-gated channels (Figure 11-12).

As might be expected from these two differences in physiological properties, the ACh-gated and voltage-gated channels are formed by distinct macromolecules that exhibit different sensitivities to drugs and toxins. Tetrodotoxin, which blocks the voltage-gated Na^+ channel, does not block the influx of Na^+ through the nicotinic ACh-gated channels. Similarly, α-bungarotoxin, a snake venom protein that binds tightly to the nicotinic receptors and blocks the action of ACh, does not interfere with voltage-gated Na^+ or K^+ channels (α-bungarotoxin has proved useful in the biochemical characterization of the ACh receptor).

In Chapter 12 we shall learn about still another type of ligand-gated channel, the *N*-methyl-D-aspartate or NMDA–type glutamate receptor, which is found in most neurons of the brain. This channel is doubly gated, responding both to voltage *and* to a chemical transmitter.

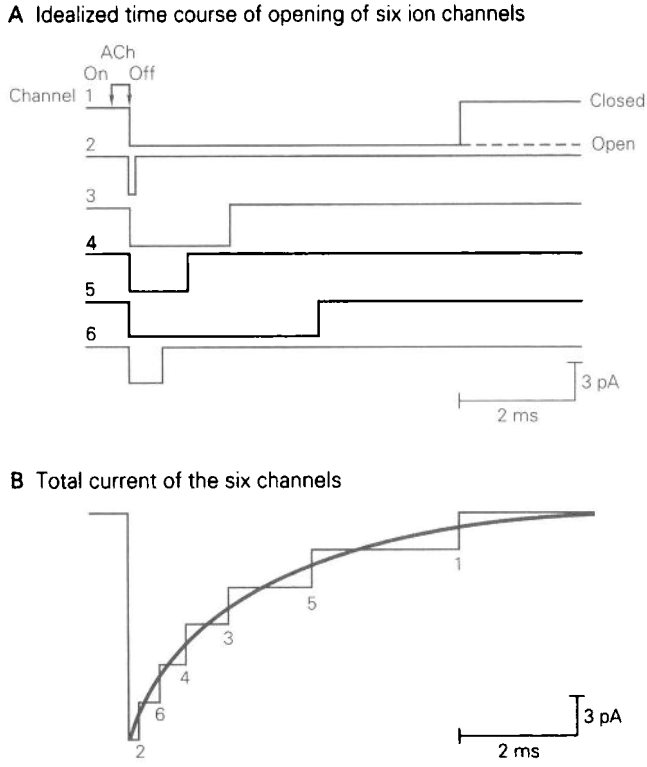

Figure 11-10 The time course of the total current at the end-plate results from the summed contributions of many individual ACh-gated channels. (Adapted from D. Colquhoun 1981.)

A. Individual ACh-gated channels open in response to a brief pulse of ACh. All channels (1-6) open rapidly and nearly simultaneously. The channels then remain open for varying durations and close at different times.

B. The stepped trace shows the sum of the six records in **A.** It reflects the sequential closing of each channel (the number indicates which channel has closed) at a hypothetical end-plate containing only six channels. In the final period of net current flow only channel 1 is open. In a current record from a whole muscle fiber, with thousands of channels, the individual channel closings are not visible because the total end-plate current (hundreds of nanoamperes) is so much larger than the single-channel current amplitude (−2.7 pA). As a result, the total end-plate current appears to decay smoothly.

A Single Macromolecule Forms the Nicotinic Acetylcholine Receptor and Channel

The nicotinic ACh-gated channel at the nerve-muscle synapse is a directly gated or ionotropic channel: the pore in the membrane through which ions flow and the binding site for the chemical transmitter (ACh) that regulates the opening of the pore are all formed by a single macromolecule. Where in the molecule is the binding site located? How is the pore formed? What are its properties? Insights into these questions have been obtained from molecular studies of the ACh-gated receptor-channel proteins and their genes.

Biochemical studies by Arthur Karlin and Jean-Pierre Changeux indicate that the mature nicotinic ACh receptor is a membrane glycoprotein formed from five subunits: two α-subunits and one β-, one γ-, and one δ-subunit (Figure 11-13). The amino terminus of each of the subunits is exposed on the extracellular surface of the membrane. The amino terminus of the α-subunit contains a site that binds ACh with high affinity. Karlin and his colleagues have demonstrated the presence of two extracellular binding sites for ACh on each channel. Those sites are formed in a cleft between each α-subunit and its neighboring γ- or δ-subunits. One molecule of ACh must bind to each of the two α-subunits for the channel to open efficiently (Figure 11-13). The inhibitory snake venom α-bungarotoxin also binds to the α-subunit.

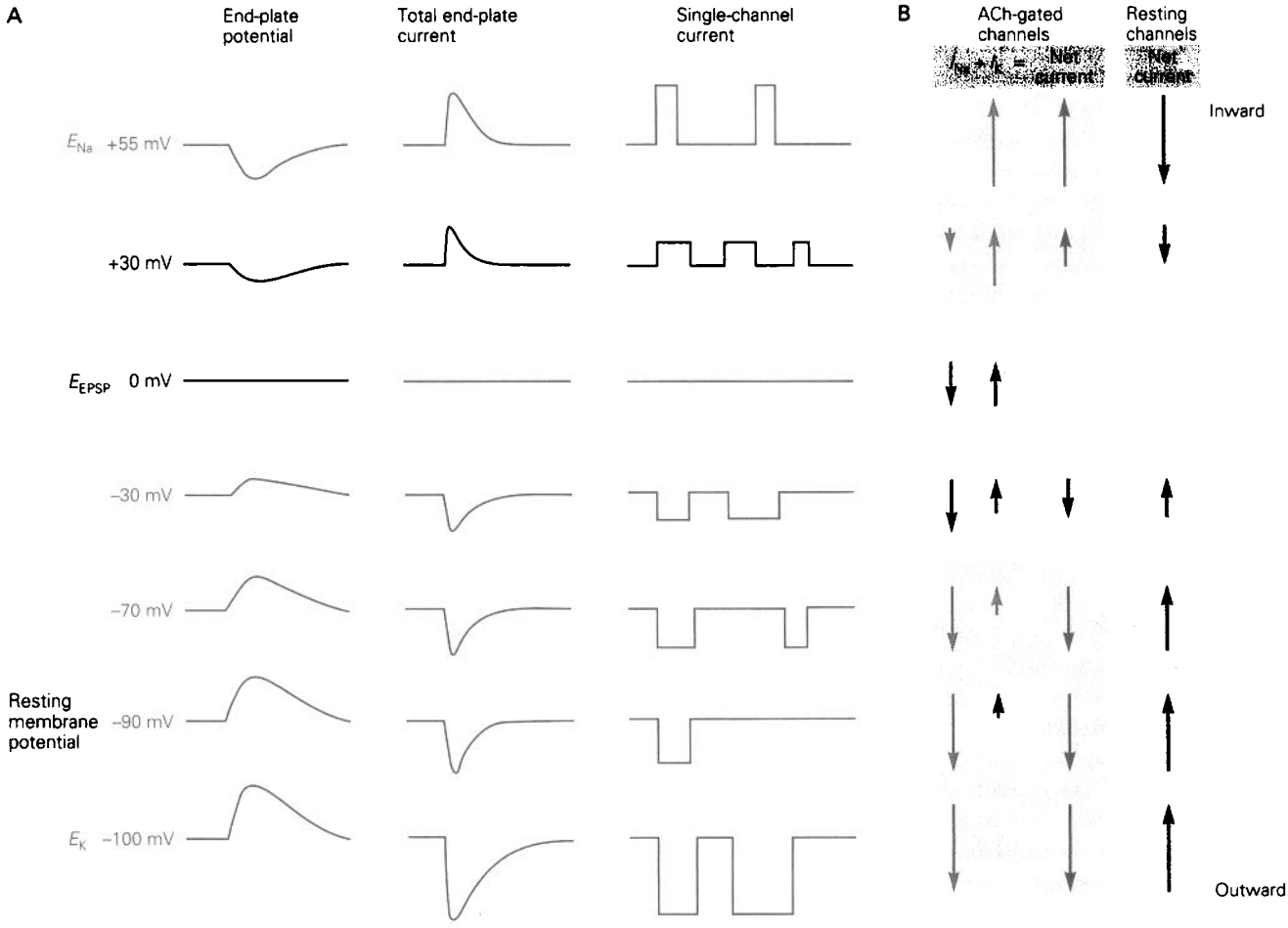

Figure 11-11 Membrane potential affects the end-plate potential, total end-plate current, and ACh-gated single-channel current in a similar way.

A. At the normal muscle resting potential of −90 mV the single-channel currents and total end-plate current (made up of currents from more than 200,0000 channels) are large and inward because of the large inward driving force on current flow through the ACh-gated channels. This large inward current produces a large depolarizing end-plate potential. At more positive levels of membrane potential (increased depolarization), the inward driving force on Na^+ is less and the outward driving force on K^+ is greater. This results in a decrease in the size of the single-channel currents and in the magnitude of the end-plate currents, thus reducing the size of the end-plate potential. At the reversal potential (0 mV) the inward Na^+ flux is balanced by the outward K^+ flux, so there is no net current flow at the end-plate and no change in V_m. Further depolarization to +30 mV inverts the direction of the end-plate current, as there is now a large outward driving force on K^+ and a small inward driving force on Na^+. As a result, the outward flow of K^+ hyperpolarizes the membrane. On either side of the reversal potential the end-plate current drives the membrane potential toward the reversal potential.

B. The direction of Na^+ and K^+ fluxes in individual channels is altered by changing V_m. The algebraic sum of the Na^+ and K^+ currents, I_{Na} and I_K, gives the *net current* that flows through the ACh-gated channels. This net synaptic current is equal in size, and opposite in direction, to that of the net extrasynaptic current flowing in the return pathway of the resting channels and membrane capacitance. (The length of each arrow represents the relative magnitude of a current.)

Insight into the structure of the channel pore has come from analysis of the primary amino acid sequences of the receptor-channel subunits as well as from biophysical studies. The work of Shosaku Numa and his colleagues demonstrated that the four subunit types are encoded by distinct but related genes. Sequence comparison of the subunits shows a high degree of similarity among them: half of the amino acid residues are identical or conservatively substituted. This similarity suggests that all subunits have a similar

structure. Furthermore, all four of the genes for the subunits are homologous; that is, they are derived from a common ancestral gene.

The distribution of the polar and nonpolar amino acids of the subunits provides important clues as to how the subunits are threaded through the membrane bilayer. Each subunit contains four hydrophobic regions of about 20 amino acids called M1–M4, each of which is thought to form an α-helix traversing the membrane. The amino acid sequences of the subunits suggest that the subunits are symmetrically arranged to create the pore through the membrane (Figure 11-14).

The walls of the channel pore are thought to be formed by the M2 region and by the segment connecting M2 to M3 (Figure 11-14B). Certain drugs that bind to one ring of serine residues and two rings of hydrophobic residues on the M2 region within the channel pore are able to inhibit current flow through the pore. Moreover, three rings of negative charge that flank the M2 region (Figure 11-15B) contribute to the channel's selectivity for cations. Each ring is made up of three or four aligned negatively charged residues contributed by different subunits.

A three-dimensional model of the ACh receptor has been proposed by Arthur Karlin and Nigel Unwin based on neutron scattering and electron diffraction images respectively (see Figure 11-3). The receptor-channel complex is divided into three regions: a large vestibule at the external membrane surface, a narrow transmembrane pore that determines cation selectivity, and a larger exit region at the internal membrane surface (Figure 11-15A). The region that extends into the extracellular space is surprisingly large, about 6 nm in length. At the external surface of the membrane the channel has a wide mouth about 2.5 nm in diameter. Within the bilayer of the membrane the channel gradually narrows.

This narrow region is quite short, only about 3 nm in length, corresponding to the length of both the M2 segment and the hydrophobic core of the bilayer (Figure 11-15B). In the open channel, the M2 segment appears to slope inward toward the central axis of the channel, so that the pore narrows continuously from the outside of the membrane to the inside (Figure 11-15C). Near the inner surface of the membrane the pore reaches its narrowest diameter, around 0.8 nm, in reasonable agreement with estimates from electrophysiological measurements. This site may correspond to the selectivity filter of the channel. At the selectivity filter, polar threonine residues extend their side chains into the lumen of the pore. The electronegative oxygen atom of the hydroxyl group may interact with the permeant cation to compensate for loss of waters of hydration. At the inner surface of the membrane, the pore suddenly widens again.

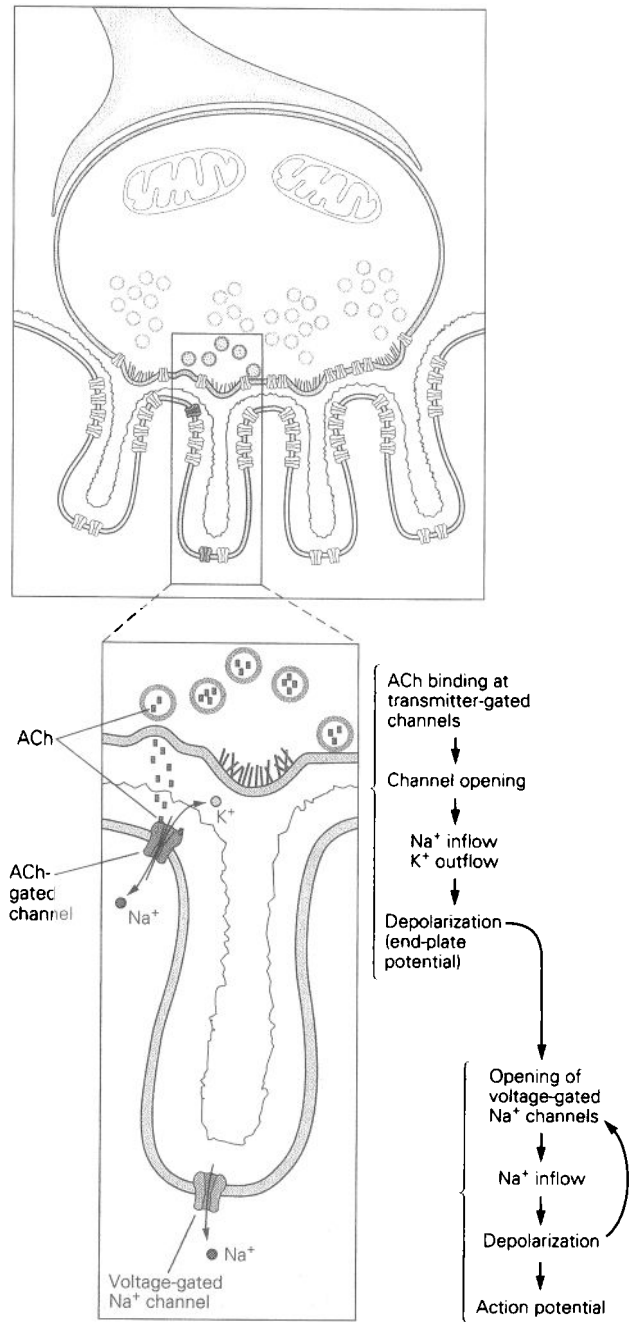

Figure 11-12 The binding of ACh in a postsynaptic muscle cell opens channels permeable to both Na^+ and K^+. The flow of these ions into and out of the cell depolarizes the cell membrane, producing the end-plate potential. This depolarization opens neighboring voltage-gated Na^+ channels in the muscle cell. To trigger an action potential, the depolarization produced by the end-plate potential must open a sufficient number of Na^+ channels to exceed the cell's threshold. (After Alberts et al. 1989.)

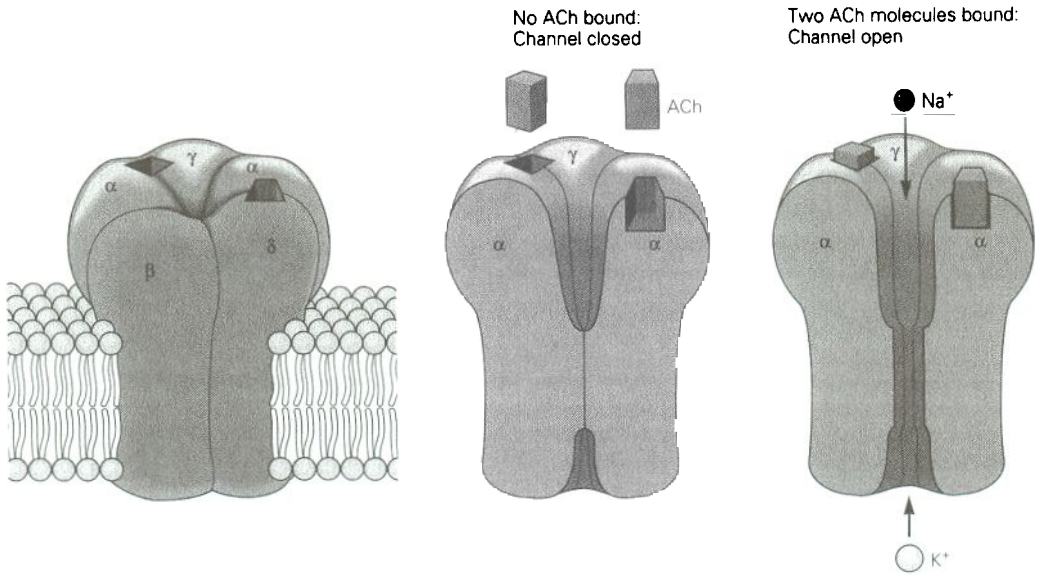

Figure 11-13 Three-dimensional model of the nicotinic ACh–gated ion channel. The receptor-channel complex consists of five subunits, all of which contribute to forming the pore. When two molecules of ACh bind to portions of the α-subunits exposed to the membrane surface, the receptor-channel changes conformation. This opens a pore in the portion of the channel embedded in the lipid bilayer, and both K^+ and Na^+ flow through the open channel down their electrochemical gradients.

On the basis of images of ACh receptors in the presence and absence of transmitter, Unwin has proposed that the M2 helix may be important for channel gating, as well as for ion permeation. His studies indicate that the M2 helix is not straight but rather has a bend or kink in its middle (Figure 11-15C). When the channel is closed, this kink projects inward toward the central axis of the pore, thereby occluding it. When the channel opens, the M2 helix rotates so that the kink lies along the wall of the channel.

A somewhat different view of the pore and gate has been provided by Karlin, who studied the reactions of small, charged reagents with amino acid side chains in the M2 segment. By comparing the ability of these compounds to react in the open and closed states of the

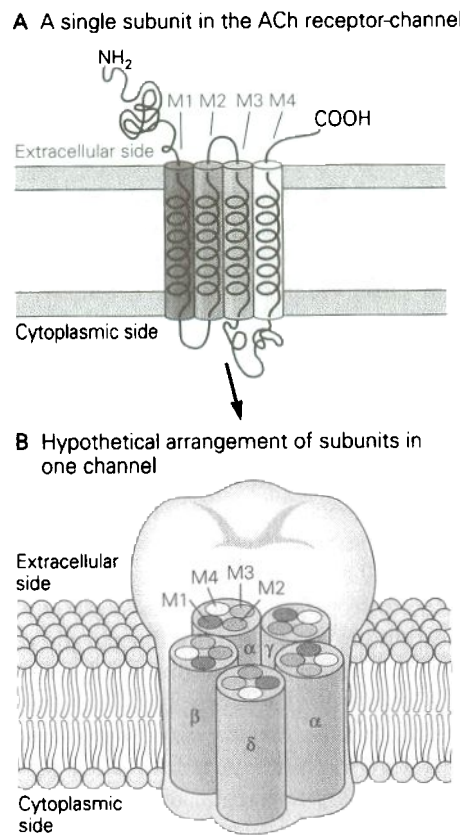

Figure 11-14 A molecular model of the transmembrane subunits of the nicotinic ACh receptor-channel.

A. Each subunit is composed of four membrane-spanning α-helices (labeled M1 through M4).

B. The five subunits are arranged such that they form an aqueous channel, with the M2 segment of each subunit facing inside and forming the lining of the pore (see turquoise cylinders, Figure 11-15A). Note that the γ-subunit lies between the two α-subunits.

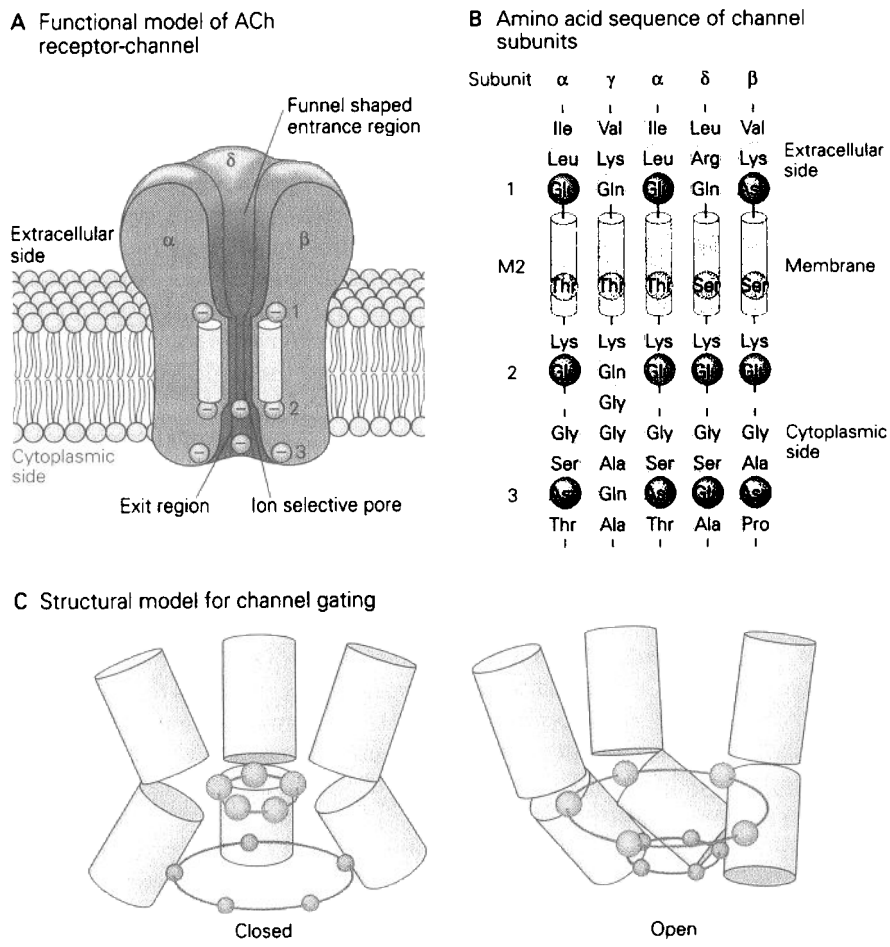

Figure 11-15 A functional model of the nicotinic ACh receptor-channel.

A. According to this model negatively charged amino acids on each subunit form three rings of charge around the pore (see part B). As an ion traverses the channel it encounters this series of negatively charged rings. The rings at the external (**1**) and internal (**3**) surfaces of the cell membrane may serve as prefilters and divalent blocking sites. The central ring (**2**) within the bilayer may contribute to the selectivity filter for cations, along with a ring of threonine and serine residues that contribute an electronegative oxygen. (Dimensions are not to scale.)

B. The amino acid sequences of the M2 and flanking regions of each of the five subunits. The horizontal series of amino acids numbered **1**, **2**, and **3** identify the three rings of negative charge (see part **A**). The position of the aligned serine and threonine residues within M2, which help form the selectivity filter, is indicated.

C. A model for gating of the ACh receptor-channel. Three of the five M2 transmembrane segments are shown. Each M2 segment is split into two cylinders, one on top of the other. **Left:** In the closed state each M2 cylinder points inward toward the central axis of the channel. A ring of five hydrophobic leucine residues (large spheres, one from each M2 segment) occludes the pore. **Right:** In the open state the cylinders tilt, thus enlarging the ring of leucines. A ring of hydrophilic threonine residues (small spheres) may form the selectivity filter near the inner mouth of the channel. (Based on Unwin 1995).

channel, Karlin concluded that the gate was at the cytoplasmic end of M2.

An Overall View

The terminals of motor neurons form synapses with muscle fibers at specialized regions in the muscle membrane called end-plates. When an action potential reaches the terminals of a presynaptic motor neuron, it causes release of ACh. The transmitter diffuses across the synaptic cleft and binds to nicotinic ACh receptors in the end-plate, thus opening channels that allow Na^+, K^+, and Ca^{2+} to flow across the postsynaptic muscle. A net influx of Na^+ ions produces a depolarizing synaptic potential called the end-plate potential.

Because the ACh-activated channels are localized to the end-plate, the opening of these channels produces only a local depolarization that spreads passively along the muscle fibers. But by depolarizing the postsynaptic cell past threshold, the transmitter-gated channels activate voltage-dependent Na^+ channels near the end-plate region. As the postsynaptic cell becomes progressively depolarized, more and more voltage-gated Na^+ channels open. In this way the Na^+ channels can quickly generate enough current to produce an actively propagated action potential.

The protein that forms the nicotinic ACh-activated channel has been purified, its genes cloned, and its amino acids sequenced. It is composed of five subunits, two of which—the α-subunits that recognize and bind ACh—are identical. Each subunit has four hydrophobic regions that are thought to form membrane-spanning α-helices.

The protein that forms the nicotinic ACh-gated channel also contains a site for recognizing and binding the ACh. This channel is thus gated directly by a chemical transmitter. The functional molecular domains of the ACh-gated channel have been identified, and the steps that link ACh-binding to the opening of the channel are now being investigated. Thus, we may soon be able to see in atomic detail the molecular dynamics of this channel's various physiological functions.

The large number of ACh-gated channels at the end-plate normally ensures that synaptic transmission will proceed with a high safety factor. In the autoimmune disease myasthenia gravis, antibodies to the ACh receptor decrease the number of ACh-gated channels, thus seriously compromising transmission at the neuromuscular junction (see Chapter 16).

Acetylcholine is only one of many neurotransmitters in the nervous system, and the end-plate potential is just one example of chemical signaling. Do transmitters in the central nervous system act in the same fashion, or are other mechanisms involved? In the past such questions were virtually unanswerable because of the small size and great variety of nerve cells in the central nervous system. However, advances in experimental technique—in particular, patch clamping—have made synaptic transmission at central synapses easier to study. Already it is clear that many neurotransmitters operate in the central nervous system much as ACh operates at the end-plate, while other transmitters produce their effects in quite different ways. In the next two chapters we shall explore some of the many variations of synaptic transmission that characterize the central and peripheral nervous systems.

Postscript: The End-Plate Current Can Be Calculated From an Equivalent Circuit

Although the flow of current through a population of ACh-activated end-plate channels can be described by Ohm's law, to understand fully how the flow of electrical current generates the end-plate potential we also need to consider all the resting channels in the surrounding membrane. Since channels are proteins that span the bilayer of the membrane, we must also take into consideration the capacitive properties of the membrane and the ionic batteries determined by the distribution of Na^+ and K^+ inside and outside the cell.

The dynamic relationship of these various components can be explained using the same rules we used in Chapter 8 to analyze the flow of current in passive electrical devices that consist only of resistors, capacitors, and batteries. We can represent the end-plate region with an equivalent circuit that has three parallel branches: (1) a branch representing the flow of synaptic current through the transmitter-gated channels; (2) a branch representing the return current flow through resting channels (the nonsynaptic membrane); and (3) a branch representing current flow across the lipid bilayer, which acts as a capacitor (Figure 11-16).

Since the end-plate current is carried by both Na^+ and K^+, we could represent the synaptic branch of the equivalent circuit as two parallel branches, each representing the flow of a different ion species. At the end-plate, however, Na^+ and K^+ flow through the same ion channel. It is therefore more convenient (and correct) to combine the Na^+ and K^+ current pathways into a single conductance, representing the channel gated by ACh. The conductance of this pathway depends on the number of channels opened, which in turn depends on the concentration of transmitter. In the absence of transmitter no channels are open and the conductance is zero. When a presynaptic action potential causes the release of transmitter, the conductance of this pathway rises to a value of around 5×10^{-6} S (or a resistance of $2 \times 10^5\ \Omega$). This is about five times the conductance of the parallel branch representing the resting or leakage channels (g_l).

The end-plate conductance is in series with a battery (E_{EPSP}), whose value is given by the reversal potential for synaptic current flow (0 mV) (Figure 11-16). This value is the weighted algebraic sum of the Na^+ and K^+ equilibrium potentials (see Box 11-1).

The current flowing during the excitatory postsynaptic potential (I_{EPSP}) is given by

$$I_{EPSP} = g_{EPSP} \times (V_m - E_{EPSP}).$$

Using this equation and the equivalent circuit of Figure 11-17 we can now analyze the end-plate potential in

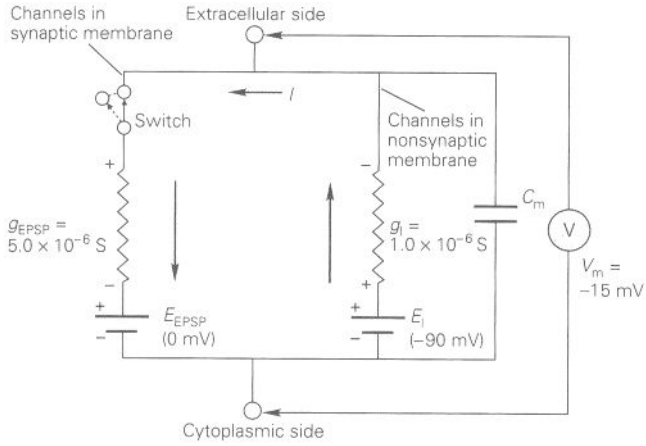

Figure 11-16 The equivalent circuit of the end-plate with two parallel current pathways. One pathway representing the synapse consists of a battery, E_{EPSP}, in series with a conductance through ACh-gated channels, g_{EPSP}. The other pathway consists of the battery representing the resting potential (E_l) in series with the conductance of the resting channels (g_l). In parallel with both of these conductance pathways is the membrane capacitance (C_m). The voltmeter (V) measures the potential difference between the inside and the outside of the cell.

When no ACh is present, the gated channels are closed and no current flows through them. This state is depicted as an open electrical circuit in which the synaptic conductance is not connected to the rest of the circuit. The binding of ACh opens the synaptic channel. This event is electrically equivalent to throwing the switch that connects the gated conductance pathway (g_{EPSP}) with the resting pathway (g_l). In the steady state current flows inward through the gated channels and outward through the resting channels. With the indicated values of conductances and batteries, the membrane will depolarize from −90 mV (its resting potential) to −15 mV (the peak of the end-plate potential).

terms of the flow of ionic current. At the onset of the excitatory synaptic action (the dynamic phase), an inward current (I_{EPSP}) flows through the ACh-activated channels because of the increased conductance to Na^+ and K^+ and the large inward driving force on Na^+ at the initial resting potential (−90 mV). Since current flows in a closed loop, the inward synaptic current must leave the cell as outward current. From the equivalent circuit we see that there are two parallel pathways for outward current flow: a conductance pathway (I_l) representing current flow through the resting (or leakage) channels and a capacitive pathway (I_c) representing current flow across the membrane capacitance. Thus,

$$I_{EPSP} = -(I_l + I_c).$$

During the earliest phase of the end-plate potential the membrane potential, V_m, is still close to its resting value, E_l. As a result, the outward driving force on current flow through the resting channels ($V_m - E_l$) is small. Therefore, most of the current leaves the cell as capacitive current and the membrane depolarizes rapidly (phase 2 in Figure 11-17). As the cell depolarizes, the outward driving force on current flow through the resting channels increases, while the inward driving force on synaptic current flow through the ACh-gated channels decreases. Concomitantly, as the concentration of ACh in the synapse falls, the ACh-gated channels begin to close, and eventually the flow of inward current through the gated channels is exactly balanced by outward current flow through the resting channels ($I_{EPSP} = -I_l$). At this point no current flows into or out of the capacitor, that is, $I_c = 0$. Since the rate of change of membrane potential is directly proportional to I_c,

$$I_c = C_m \times \Delta V/\Delta t,$$

the membrane potential will have reached a peak steady-state value, $\Delta V/\Delta t = 0$ (phase 3 in Figure 11-17).

As the gated channels close, I_{EPSP} decreases further. Now I_{EPSP} and I_l are no longer in balance and the membrane potential starts to repolarize, because the outward current flow due to I_l becomes larger than the inward synaptic current. During most of the declining phase of the synaptic action, current no longer flows through the ACh-gated channels since all these channels are closed. Instead, current flows out only through the resting channels and in across the capacitor (phase 4 in Figure 11-17).

When the end-plate potential is at its peak or steady-state value, $I_c = 0$ and therefore the value of V_m can be easily calculated. The inward current flow through the gated channels (I_{EPSP}) must be exactly balanced by outward current flow through the resting channels (I_l):

$$I_{EPSP} + I_l = 0. \qquad \textbf{(11-8)}$$

The current flowing through the active ACh-gated channels (I_{EPSP}) and through the resting channels (I_l) is given by Ohm's law:

$$I_{EPSP} = g_{EPSP} \times (V_m - E_{EPSP}),$$

and

$$I_l = g_l \times (V_m - E_l).$$

By substituting these two expressions into Equation 11-8, we obtain

$$g_{EPSP} \times (V_m - E_{EPSP}) + g_l \times (V_m - E_l) = 0.$$

To solve for V_m we need only expand the two products in the equation and rearrange them so that all terms in

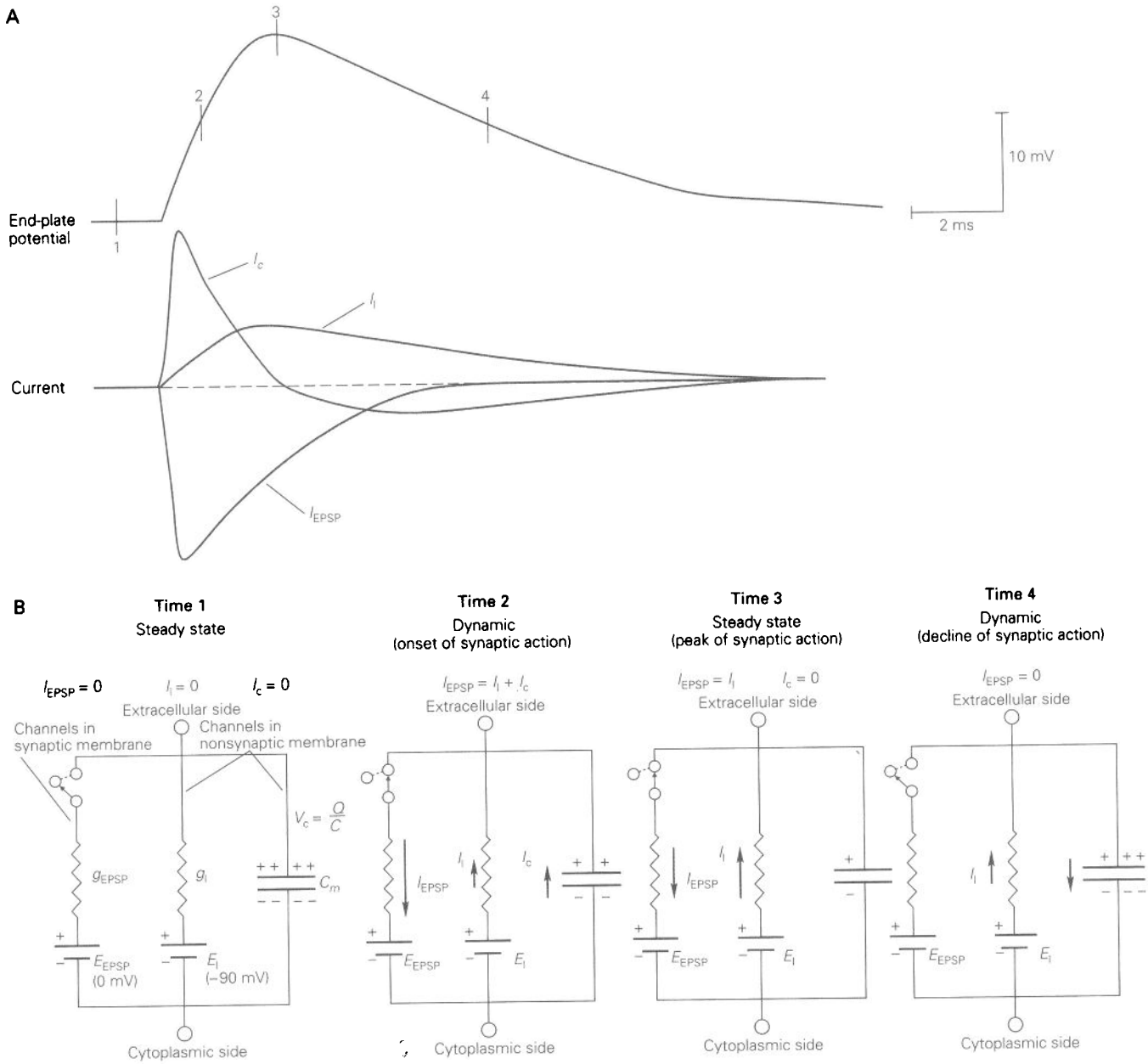

Figure 11-17 Both the ACh-gated synaptic conductance and the passive membrane properties of the muscle cell determine the time course of the end-plate potential.

A. Comparison of the time course of the end-plate potential (**top trace**) with the time courses of the component currents through the ACh-gated channels (I_{EPSP}), the resting (or leakage) channels (I_l), and the capacitor (I_c). Capacitive current flows only when the membrane potential is changing. In the steady state, such as at the peak of the end-plate potential, the inward flow of ionic current through the ACh-gated channels is exactly balanced by the outward flow of ionic current across the resting channels, and there is no flow of capacitive current.

B. Equivalent circuits for the current at times 1, 2, 3, and 4 shown in part **A.** (The relative magnitude of a current is represented by the length of the arrows.)

voltage (V_m) appear on the left side:

$$(g_{EPSP} \times V_m) + (g_l \times V_m) = (g_{EPSP} \times E_{EPSP}) + (g_l \times E_l).$$

By factoring out V_m on the left side, we finally obtain

$$V_m = \frac{(g_{EPSP} \times E_{EPSP}) + (g_l \times E_l)}{g_{EPSP} + g_l}. \quad \textbf{(11-9)}$$

This equation is similar to that used to calculate the resting and action potentials (Chapter 7). According to Equation 11-9, the peak voltage of the end-plate potential is a weighted average of the electromotive forces of the two batteries for gated and resting currents. The weighting factors are given by the relative magnitude of the two conductances. If the gated conductance is much smaller than the resting membrane conductance ($g_{EPSP} \ll g_l$), $g_{EPSP} \times E_{EPSP}$ will be negligible compared with $g_l \times E_l$. Under these conditions, V_m will remain close to E_l. This situation occurs when only a few channels are opened by ACh (because its concentration is low). On the other hand, if g_{EPSP} is much larger than g_l, Equation 11-9 states that V_m approaches E_{EPSP}, the synaptic reversal potential. This situation occurs when the concentration of ACh is high and a large number of ACh-activated channels are open. At intermediate ACh concentrations, with a moderate number of ACh-activated channels open, the peak end-plate potential lies somewhere between E_l and E_{EPSP}.

We can now use this equation to calculate the peak end-plate potential for the specific case shown in Figure 11-16, where $g_{EPSP} = 5 \times 10^{-6}$ S, $g_l = 1 \times 10^{-6}$ S, $E_{EPSP} = 0$ mV, and $E_l = -90$ mV. Substituting these values into Equation 11-9 yields

$$V_m = \frac{[(5 \times 10^{-6}\,\text{S}) \times (0\,\text{mV})] + [(1 \times 10^{-6}\,\text{S}) \times (-90\,\text{mV})]}{(5 \times 10^{-6}\,\text{S}) + (1 \times 10^{-6}\,\text{S})}.$$

or

$$V_m = \frac{(1 \times 10^{-6}\,\text{S}) \times (-90\,\text{mV})}{(6 \times 10^{-6}\,\text{S})}$$

$$= -15\,\text{mV}.$$

The peak amplitude of the end-plate potential is then

$$\Delta V_{EPSP} = V_m - E_l$$

$$= -15\,\text{mV} - (-90\,\text{mV})$$

$$= 75\,\text{mV}.$$

As a check for consistency we can see whether, at the peak of the end-plate potential, the synaptic current is equal and opposite to the nonsynaptic current so that the net membrane current is indeed equal to zero:

$$I_{EPSP} = (5 \times 10^{-6}\,\text{S}) \times (-15\,\text{mV} - 0\,\text{mV})$$

$$= -75 \times 10^{-9}\,\text{A}$$

and

$$I_l = (1 \times 10^{-6}\,\text{S}) \times [-15\,\text{mV} - (-90\,\text{mV})],$$

$$= 75 \times 10^{-9}\,\text{A}.$$

Here we see that Equation 11-9 ensures that $I_{EPSP} + I_l = 0$.

Eric R. Kandel
Steven A. Siegelbaum

Selected Readings

Fatt P, Katz B. 1951. An analysis of the end-plate potential recorded with an intra-cellular electrode. J Physiol (Lond) 115:320–370.

Heuser JE, Reese TS. 1977. Structure of the synapse. In: ER Kandel (ed), *Handbook of Physiology: A Critical, Comprehensive Presentation of Physiological Knowledge and Concepts*, Sect. 1, *The Nervous System*. Vol. 1, *Cellular Biology of Neurons*, Part 1, pp. 261–294. Bethesda, MD: American Physiological Society.

Hille B. 1992. In: *Ionic Channels of Excitable Membranes*, 2nd ed, pp. 140–169. Sunderland, MA: Sinauer.

Imoto K, Busch C, Sakmann B, Mishina M, Konno T, Nakai J, Bujo H, Mori Y, Fukuda K, Numa S. 1988. Rings of negatively charged amino acids determine the acetylcholine receptor-channel conductance. Nature 335:645–648.

Karlin A, Akabas MH. 1995. Toward a structural basis for the function of nicotinic acetylcholine receptors and their cousins. Neuron 15:1231–1244.

Neher E, Sakmann B. 1976. Single-channel currents recorded from membrane of denervated frog muscle fibres. Nature 260:799–802.

Unwin N. 1993. Neurotransmitter action: opening of ligand-gated ion channels. Cell 72(Suppl):31–41.

References

Akabas MH, Kaufmann C, Archdeacon P, Karlin A. 1994. Identification of acetylcholine receptor-channel–lining residues in the entire M2 segment of the α-subunit. Neuron 13:919–927.

Alberts B, Bray D, Lewis J, Raff M, Roberts K, Watson JD. 1989. *Molecular Biology of the Cell*, 2nd ed. New York: Garland.

Charnet P, Labarca C, Leonard RJ, Vogelaar NJ, Czyzyk L, Gouin A, Davidson N, Lester HA. 1990. An open channel

blocker interacts with adjacent turns of α-helices in the nicotinic acetylcholine receptor. Neuron 4:87–95.

Claudio T, Ballivet M, Patrick J, Heinemann S. 1983. Nucleotide and deduced amino acid sequences of *Torpedo californica* acetylcholine receptor γ-subunit. Proc Natl Acad Sci U S A 80:1111–1115.

Colquhoun D. 1981. How fast do drugs work? Trends Pharmacol Sci 2:212–217.

Dwyer TM, Adams DJ, Hille B. 1980. The permeability of the endplate channel to organic cations in frog muscle. J Gen Physiol 75:469–492.

Fertuck HC, Salpeter MM. 1974. Localization of acetylcholine receptor by ^{125}I-labeled α-bungarotoxin binding at mouse motor endplates. Proc Natl Acad Sci U S A 71:1376–1378.

Heuser JE, Salpeter SR. 1979. Organization of acetylcholine receptors in quick-frozen, deep-etched, and rotary-replicated *Torpedo* postsynaptic membrane. J Cell Biol 82:150–173.

Ko C-P. 1984. Regeneration of the active zone at the frog neuromuscular junction. J Cell Biol 98:1685–1695.

Kuffler SW, Nicholls JG, Martin AR. 1984. *From Neuron to Brain: A Cellular Approach to the Function of the Nervous System*, 2nd ed. Sunderland, MA: Sinauer.

McMahan UJ, Kuffler SW. 1971. Visual identification of synaptic boutons on living ganglion cells and of varicosities in postganglionic axons in the heart of the frog. Proc R Soc Lond B Biol Sci 177:485–508.

Miles FA. 1969. *Excitable Cells*. London: Heinemann.

Noda M, Furutani Y, Takahashi H, Toyosato M, Tanabe T, Shimizu S, Kikyotani S, Kayano T, Hirose T, Inayama S, Numa S. 1983. Cloning and sequence analysis of calf cDNA and human genomic DNA encoding α-subunit precursor of muscle acetylcholine receptor. Nature 305:818–823.

Noda M, Takahashi H, Tanabe T, Toyosato M, Kikyotani S, Furutani Y, Hirose T, Takashima H, Inayama S, Miyata T, Numa S. 1983. Structural homology of *Torpedo californica* acetylcholine receptor subunits. Nature 302:528–532.

Palay SL. 1958. The morphology of synapses in the central nervous system. Exp Cell Res Suppl 5:275–293.

Raftery MA, Hunkapiller MW, Strader CD, Hood LE. 1980. Acetylcholine receptor: complex of homologous subunits. Science 208:1454–1457.

Revah F, Galzi J-L, Giraudat J, Haumont PY, Lederer F, Changeux J-P. 1990. The noncompetitive blocker [^{3}H]chlorpromazine labels three amino acids of the acetylcholine receptor gamma subunit: implications for the alpha-helical organization of regions MII and for the structure of the ion channel. Proc Natl Acad Sci U S A 87:4675–4679.

Takeuchi A. 1977. Junctional transmission. I. Postsynaptic mechanisms. In: ER Kandel (ed), *Handbook of Physiology: A Critical, Comprehensive Presentation of Physiological Knowledge and Concepts*, Sect. 1, *The Nervous System*. Vol. 1, *Cellular Biology of Neurons*, Part 1, pp. 295–327. Bethesda, MD: American Physiological Society.

Toyoshima C, Unwin N. 1988. Ion channel of acetylcholine receptor reconstructed from images of postsynaptic membranes. Nature 336:247–250.

Verrall S, Hall ZW. 1992. The N-terminal domains of acetylcholine receptor subunits contain recognition signals for the initial steps of receptor assembly. Cell 68:23–31.

Villarroel A, Herlitze S, Koenen M, Sakmann B. 1991. Location of a threonine residue in the alpha-subunit M2 transmembrane segment that determines the ion flow through the acetylcholine receptor-channel. Proc R Soc Lond B Biol Sci 243:69–74.

Unwin N. 1995. Acetylcholine receptor-channel imaged in the open state. Nature 373:37–43.